Effect of rail unevenness correlation on the prediction of ground-borne vibration from railways

Evangelos Ntotsios; David Thompson
Institute of Sound and Vibration Research, University of Southampton, Southampton, SO17 1BJ, U.K.

Mohammed Hussein
Civil & Architectural Engineering Department, Qatar University, Doha, Qatar.

Summary
This paper presents the influence of rail unevenness correlation on the predicted track and ground vibration. The study is based on an integrated railway model in the wavenumber-frequency domain with varying complexity describing the dynamic system of a ballasted track on layered elastic half-space. In order to investigate how ground vibration levels are influenced by taking into account different correlation levels between the two rails, the traction variation across the track-ground interface is included and the track model is discretised laterally including both rails separately and allowing for the pitching motion of the sleepers. The paper presents the effect of the different modelling approaches on the response predictions and compares the dynamic response calculated for a range of model/excitation parameters.

PACS no. 43.50.Lj, 43.40.At

1. Introduction

An important issue regarding the environmental impact of existing and future railway lines is the problem of ground vibration induced by the trains running on surface railways or in tunnels. The vibration is generated at the wheel-rail interface due to the passage of individual wheels along tracks (quasi-static loading) and due to irregularities of wheels and tracks (dynamic loading). The generated vibration is a problem because it propagates through the ground to nearby buildings where it may cause annoyance to people and malfunctioning of sensitive equipment. Inhabitants of buildings perceive vibration either directly, due to motion of floors and walls, or indirectly as re-radiated noise.
A large number of semi-analytical, numerical and empirical models for predicting vibration from surface and underground railways have been presented in the literature throughout the decades of studying ground-borne vibration. The predictions of these models are essential for understanding the physics of vibration generation and propagation. These models range from simple multi-degree-of-freedom models to two-dimensional and more comprehensive three-dimensional models. A comprehensive overview of the state of the art on railway induced ground vibration models can be found in [1].
Several of these models are developed by coupling sub-models for the train, the track and the soil and are all based at some extent upon simplifying assumptions. The nature and extent of these simplifying assumptions that are introduced in the modelling effort may depend on the engineering insight to replicate the operational condition of interest, the lack of complete data for the simulation, or the computational power needed for the realization. Although essential for the realization of the modelling effort, these simplifying assumptions introduce inaccuracies and uncertainties into the predictions, which in many cases remain unquantified.
This paper investigates one commonly used assumption in modelling of ground-borne vibration, namely that the unevenness of the two rails can be treated as fully correlated. Unevenness measurements from two operational tracks are reported in order to investigate the spectral content correlation of the two rails. Next, a surface railway model with varying complexity describing the dynamic system of a ballasted track on layered

elastic half-space is presented. The model can take into account the traction variation across the track-ground interface similarly with [2] while the track is discretised laterally including both rails separately allowing the different correlation levels between the two rails. The effect of the assumption is illustrated by calculating and comparing the dynamic response predictions for a range of model/excitation parameters.

2. Unevenness correlation between the rails

For the majority of models predicting ground-borne vibration in the literature the two rails and wheels are considered to have identical vibration. Even where the bending of the whole sleeper is included it is usually assumed that the excitation is symmetrical on the two rails. At higher frequencies typical of rolling noise it is usually assumed that the roughness on the two rails is uncorrelated. Thus the mean-square responses, due to excitation on the two rails can be added [3].

There is not enough information about the correlation between the roughness on two rails of a track or two wheels of a wheelset. However, it appears a reasonable assumption that they can be treated as uncorrelated at short wavelengths. Measurements of track geometry at very long wavelengths exist from track measuring coaches. In Figure 1, the track geometry measurements with such a measurement train are shown for two operational U.K. railway tracks. The left one is a typical ballasted track and the right is a slab track. The one-third octave band rail unevenness is estimated for both rails and the coherence function between the left and right rail profiles is shown, where the coherence function provides a spectral quantification of the correlation between the unevenness of the two rails. It can be seen that although the rail unevenness level is similar for both rails for wavelengths longer than 2 m, the coherence function shows that there is a strong correlation (high coherence value) between the two rails for wavelengths longer than 4 m for than ballasted track and 10 m for the slab track.

In general, it seems reasonable to assume that wavelengths shorter than about 0.6 m, which is the typical sleeper spacing, can be treated as correlated between the two rails. Wavelengths longer than 0.6 m should be treated as uncorrelated inputs. These components of low frequency excitation are relevant to ground-borne vibration and also often important for feelable vibration. Nevertheless, discrete features such as wheel flats or rail joints are likely to be strongly correlated between the two rails even for quite short wavelengths.

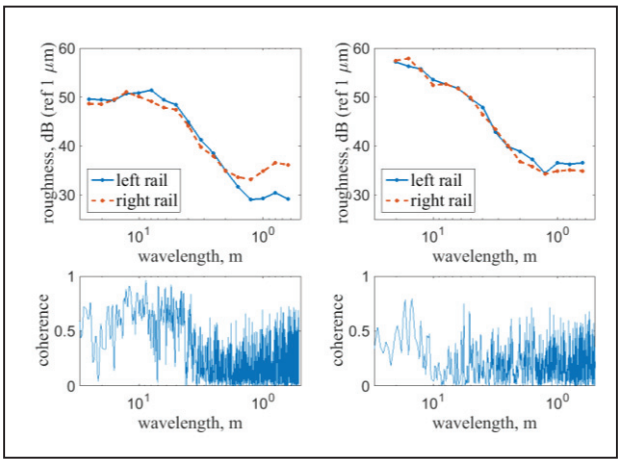

Figure 1. Unevenness spectrum of left and right rail in one third octave bands (top) and coherence function (bottom) for a ballasted (left) and a slab track (right).

3. Numerical model

The model that is used to investigate the dynamic response of a surface ballasted track railway system is shown in Figure 2. In the longitudinal direction of the track, the geometry of the track and the soil is assumed to be invariant. The railway track is aligned in the x direction and has an invariant contact width $2b$ with the ground. Different railway structures may be represented by different models having the same form. In this work, a track structure comprising rail, rail pad, sleeper and ballast is presented (see Figure 3).

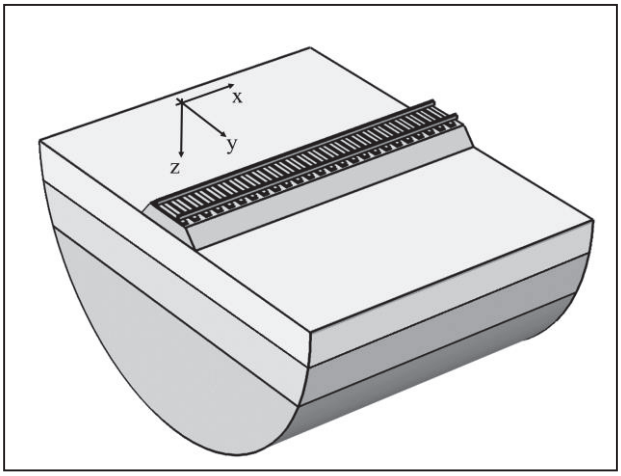

Figure 2. Model for the track/ground system

The model is formulated in the wavenumber-frequency domain and uses as inputs the moving

train axle loads and the Power Spectral Density (PSD) of the rail unevenness in terms of the wavenumber along the railway track. An extension of the semi-analytical model developed by Sheng et al. in [3] is used for the prediction of the ground response excited by moving harmonic loads acting via the coupled track structure. The model which is based on the flexibility matrix approach uses the Fourier transform in the wavenumber domain β, γ with respect to the coordinates x, y along and normal to the track.

When using the assumption that the roughness on both rails is correlated a track model with a single rail can be used as shown in Figure 3(a). In this case, in the longitudinal direction, the two rails are represented as a single Euler-Bernoulli beam and the rail pads are modelled as a distributed vertical stiffness. The sleepers are modelled as a continuous mass per unit length of the track and the ballast is modelled as continuous distributed vertical spring stiffness with consistent mass. An embankment, if present, can be modeled in the same way as the ballast. The coupling of the ground with the railway track is carried out by taking into account the continuity of the displacements on the track centreline and the equilibrium of the homogeneous stress distribution in the plane of contact between them.

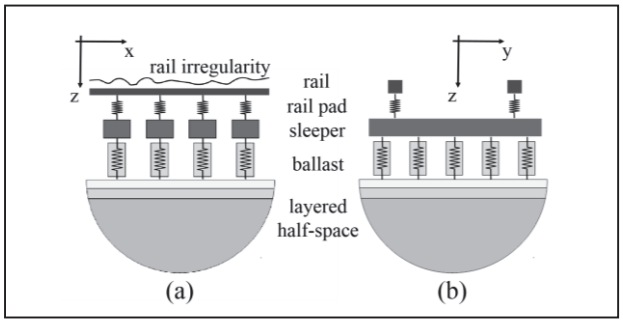

Figure 3. Longitudinal (a) and lateral (b) discretization of the track.

When a train is considered in the model, the coupling of a wheelset with the rails is achieved by decomposing the vertical profile of the rail into a spectrum of discrete harmonic components. A single harmonic component is denoted by $w(x) = Ae^{i(2\pi/\lambda)x}$ where λ denotes the wavelength and A the amplitude which may be complex. The relation between the angular frequency of the dynamic loading and the wavelength of the rail irregularity is $\omega = 2\pi v/\lambda$, where v is the speed of the train.

3.1. Track lateral discretization

When loaded, the track exerts a load on the half-space. Therefore, a contact force F_G between track and soil is introduced (F_G has the dimension of force per unit of length). In a following step, the interface conditions are discretised. The discretisation will introduce a finite sum of the normal tractions at the track/ground interface. The principle is shown in Figure 4. Across the interface, the continuous variable y is changed into a discrete variable y_j, positioned at the middle of an interval N with width Δ. Within each subdomain j, stresses are assumed to be invariant. The displacement compatibility is required along the lines $y = y_j$ Coordinate y_j is defined as $y_j = -b + \Delta(2j-1)/2$ where $1 \le j \le N$ with $N = 2b/\Delta$. For $N = 1$ the homogeneous stress distribution results, with compatibility along the centre-line.

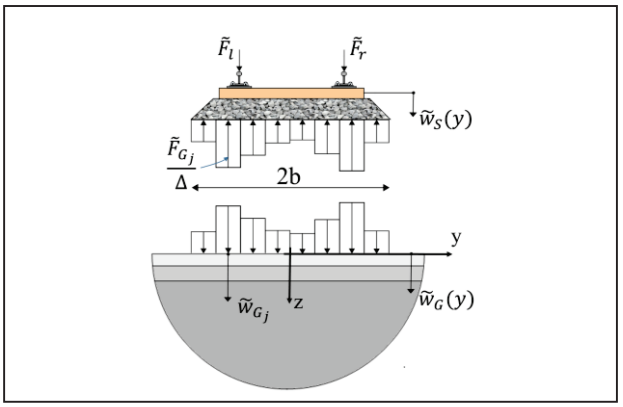

Figure 4. Assumed interface conditions and discretisation of the stress field across the track-soil interface.

The displacement of a point on the ground within the jth strip can be calculated, using the Green's function for the layered half-space, as the superposition of the displacements of that point due to the individual excitation at all strips as follows

$$\tilde{w}_{G_j}(\beta, y_j) = \sum_{i=1}^{N} \tilde{H}_G(\beta, y_{i,j}) \tilde{F}_{G_i} \qquad (1)$$

where $\tilde{H}_G(\beta, y_{i,j})$ is the transfer function of a point at strip j, that is at a distance $y_{i,j}$ from strip i, due to a unit excitation at strip i, with $y_{i,j} \ge 0$ when $i \le j$ and $y_{i,j} < 0$ otherwise.

The transfer functions of the ground in the wavenumber domain, $\tilde{H}_G(\beta, \gamma)$, are calculated using the Green's functions for a layered half-space due a unit load acting downwards at $y = 0$

and these are given in [4]. To calculate $\widetilde{H}_G(\beta, y_{i,j})$ therefore, the inverse Fourier transformation from the γ domain to the y domain should be calculated as

$$\widetilde{H}_G(\beta, y) = \frac{1}{2\pi}\int_{-\infty}^{\infty} \widetilde{H}_G(\beta,\gamma) e^{i\gamma y} d\gamma \qquad (2)$$

The transfer function of the ground due to a strip load of width Δ and constant magnitude $1/\Delta$, distributed symmetrically about $y = 0$, can be calculated by weighting $\widetilde{H}_G(\beta,\gamma)$ by a factor corresponding to the transformation of the strip to the wavenumber domain; i.e. by $\frac{\sin(\gamma\Delta/2)}{\Delta/2}$.

Applying this to the jth strip and due to symmetry in the γ domain results in

$$\widetilde{H}_G(\beta, y_{i,j}) = \frac{1}{2\pi}\int_{0}^{\infty} \widetilde{H}_G(\beta,\gamma)\frac{\sin(\gamma\Delta/2)}{\Delta/2}\cos(\gamma y_{i,j}) d\gamma \quad (3)$$

Equation 3 can be formulated for all the strips and the resulting system of equations dropping β for brevity can be written in matrix form as

$$\widetilde{\mathbf{w}}_G = \widetilde{\mathbf{H}}_G \widetilde{\mathbf{F}}_G \qquad (4)$$

Where $\widetilde{\mathbf{H}}_G$ is an $N \times N$ matrix of the form

$$\widetilde{\mathbf{H}}_G = \begin{bmatrix} \widetilde{H}_G(0) & \widetilde{H}_G(-\Delta) & \cdots & \widetilde{H}_G(-(N-1)\Delta) \\ \widetilde{H}_G(-\Delta) & \widetilde{H}_G(0) & \cdots & \widetilde{H}_G(-(N-2)\Delta) \\ \vdots & \vdots & \ddots & \vdots \\ \widetilde{H}_G(-(N-1)\Delta) & \widetilde{H}_G(-(N-2)\Delta) & \cdots & \widetilde{H}_G(0) \end{bmatrix} \qquad (5)$$

and the vectors $\widetilde{\mathbf{w}}_G = \begin{bmatrix}\widetilde{w}_{G_1} & \widetilde{w}_{G_2} & \dots & \widetilde{w}_{G_N}\end{bmatrix}^{\mathrm{T}}$ and $\widetilde{\mathbf{F}}_G = \begin{bmatrix}\widetilde{F}_{G_1} & \widetilde{F}_{G_2} & \dots & \widetilde{F}_{G_N}\end{bmatrix}^{\mathrm{T}}$ contain the displacements and forces respectively for all N strips.

For the jth strip the mutual force at the track/ground interface can be expressed, in the wavenumber-frequency domain, as

$$\widetilde{F}_{G_j}(\beta, y_j) = k_B \Delta\left\{\widetilde{w}_S(\beta) - \widetilde{w}_{G_j}(\beta, y_j)\right\} \qquad (6)$$

where $\widetilde{w}_S(\beta)$ is the displacement of the sleeper and $k_B\Delta$ is the stiffness magnitude of the ballast for any one strip.

3.2. Sleeper and ground response

By allowing the pitching motion around the x axis (along the track) for a rigid sleeper with polar moment of inertia J_x, the displacement of the sleeper in the lateral direction can be written as a function of y_j

$$\widetilde{w}_S(\beta, y) = \widetilde{w}_S(\beta, y_j) = \widetilde{w}_{S0}(\beta) - y_j\widetilde{\theta}_S(\beta) \qquad (7)$$

where $\widetilde{w}_{S0}$ is the displacement of the centre of mass (at $y = 0$) of the sleeper and $\tilde{\theta}_S$ is the angle of rotation around the x axis of the sleeper. Thus, equation 6 can be written as

$$\widetilde{F}_{G_j}(\beta, y_j) = k_B\Delta\left\{\widetilde{w}_{S0}(\beta) - y_j\widetilde{\theta}_S(\beta) - \widetilde{w}_{G_j}(\beta, y_j)\right\} \qquad (8)$$

The above formulation allows the modelling of two separate rails on the track. The force delivered from each rail through the rail pads of stiffness k_P to the sleeper can be written as

$$\begin{aligned} \widetilde{F}_{R,left}(\beta) &= k_P\left\{\widetilde{w}_{S0}(\beta) + b_R\widetilde{\theta}_S(\beta) - \widetilde{w}_{R,left}(\beta)\right\} \\ \widetilde{F}_{R,right}(\beta) &= k_P\left\{\widetilde{w}_{S0}(\beta) - b_R\widetilde{\theta}_S(\beta) - \widetilde{w}_{R,right}(\beta)\right\} \end{aligned} \qquad (9)$$

where k_P is half the track gauge and $\widetilde{w}_{R,left}$ $\widetilde{w}_{R,right}$ are the displacement of the left and the right rail respectively in the wavenumber domain.

Using the Fourier transformed equations of motion for the rails, the sleeper and the ballast leads to a system of linear equations similarly with [3]. In the equations the internal forces can be substituted from equations 8 and 9. The track/ground coupling force can be applied using equation 4 and the external loading can be directly applied on each rail. The solution of the system will give the responses of the rails, the sleeper and the force applied on the ground for each wavenumber β.

Once the contact force profile has been calculated, it can be used as excitation to the ground model in order to calculate the ground response, $\widetilde{w}_{G_j}(\beta, y)$ at a distance y from the y-origin. The total response at this point is then a superposition of its responses due to excitations at all the strips. Hence, the total distance from the point to the jth strip will be $y - y_j$.

4. Numerical results and comparison

This section investigates the differences in the response of the model by comparing the predictions using different modelling approaches for a set of practical railway parameters. In all simulations the same soil and track parameters were used and they are reported in [6]. First, the efficiency of the lateral discretization of the track/ground interface is evaluated. Next, the effect of different excitation correlation on the two rails is investigated; and finally, the assumption that the total response can be treated as a superposition of the responses of each rail separately by assuming that the roughness on both rails is uncorrelated is investigated through a simulations of a train pass-by.

4.1. The influence of different interface descriptions between the track and the ground

In order to highlight the efficiency of the lateral discretization of the track/ground interface presented in Section 3.1, the response predicted by the model is compared for different interface conditions. The assumed homogeneous load distribution in the plane of contact between the track and the ground is compared with a discretized loading of $N = 20$ strips. For the application, the track is loaded by a unit moving harmonic load with a speed of 150 km/h and the response is calculated on the track components and at the free-field.

Figure 5(a), shows the comparison between the loading profile of the track/ground interface for uniform $(N = 1)$ and a discretized $(N = 20)$ loading at 4 and at 60 Hz. The predicted ground response with distance y from the track for the four cases is shown in Figure 5(b). It can be seen that for the low frequency excitation (longer track unevenness wavelengths) the vibration level on the ground at all distances is similar for the two loading conditions. For the higher frequency excitation case though, there is about a 4 dB constant underestimation of the vibration level predicted away from the track when using the assumption of a uniform track/ground loading.

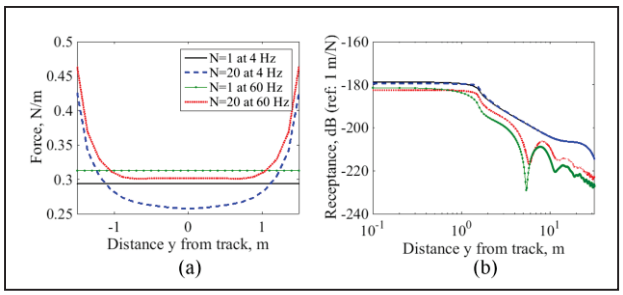

Figure 5. (a) Track/ground interaction force magnitude profiles and (b) receptance magnitude at the ground.

For exploring further the effect of the loading interface in a wider excitation frequency spectrum, the track and ground response was calculated for moving loads of 150 km/h with excitation in the frequency range 0 to 100 Hz. Figure 6, shows the predicted rail and ground receptance magnitude at $y = 0$ (at the centre-line) and at $y = 16$ m from the track. The results for the two loading cases are similar, apart from a dip of the ground response at $y = 16$ m, that appears for frequencies 50 to 95 Hz. This dip causes an underestimation of up to 17 dB at around 73 Hz of the vibration level for the uniform loading. It is caused by the fixed width of the uniform load applied by the track on the ground, $2b = 3.2$ m for this track. At this frequency, this distance corresponds to the Rayleigh wavelength at this site.

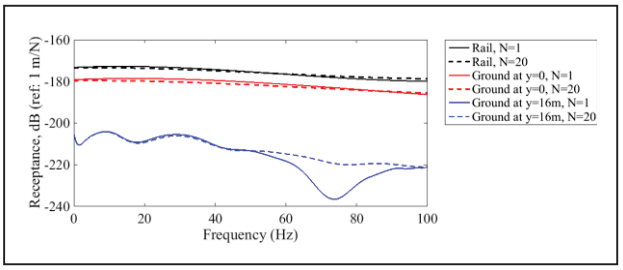

Figure 6. Receptance magnitude at y=0 and y=16 m.

4.2. The influence of rail input correlation

In this example the effect of the assumption that the rail roughness is correlated between the two rails is investigated. The application uses the formulation presented in section 3.2 where the sleeper is modelled as a rigid body that can rotate around the x axis allowing different loading conditions on the two rails.

Three different loading conditions on the rails are presented. In the first case, the loading of the two rails is considered as in-phase $(\phi = 0)$. For the second case, the loading on the two rails is antiphase $(\phi = \pi$ rad); and for the third case the difference in the phase loading between the left and the right rail is considered out-of-phase with $\phi = \pi/2$. The track/ground loading interface is considered as $N = 20$ strips.

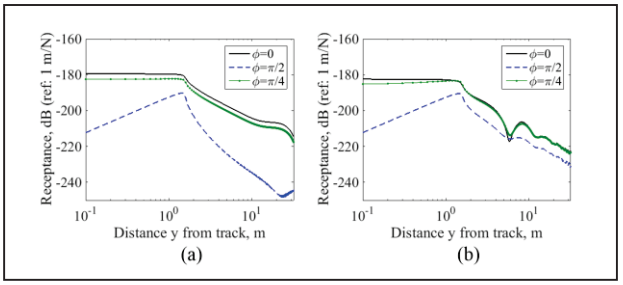

Figure 7. Receptance magnitude for excitation of (a) 4 Hz and (b) 60 Hz.

Figure 7, shows the comparison between the three loading cases of the predicted receptance magnitude with distance y. Similarly with the example in 4.1, the load moves on the track with speed of 150 km/h and two excitation frequencies are considered, 4 Hz and 60 Hz. It can be seen that for the case of out-of-phase loading the pitching motion of the sleeper is dominant and significantly decreases the vibration level predictions on the ground. For the case of $\phi = \pi/2$ difference in the

phase of the loading, the influence of the pitching motion of the sleeper is smaller and the response is about 3 dB lower compared with the in-phase loading for 4 Hz at all distances and below the track for the 60 Hz case.

Next, the assumption that the total response can be treated as a superposition of the responses of each rail separately by assuming that the roughness on both rails is uncorrelated was explored. For this, a simulation of a train pass-by with two different track loading conditions was performed. In the first case, the pass-by response is calculated by using the same dynamic loading on both rails simultaneously, as above. In the second case, the response is calculated by applying the dynamic loading on each rail separately and the overall response is calculated by adding the response due to the loading on each rail. In the latter case the pitching motion of the sleeper is included. The train properties and the rail unevenness profile for the simulations used can be found in [6].

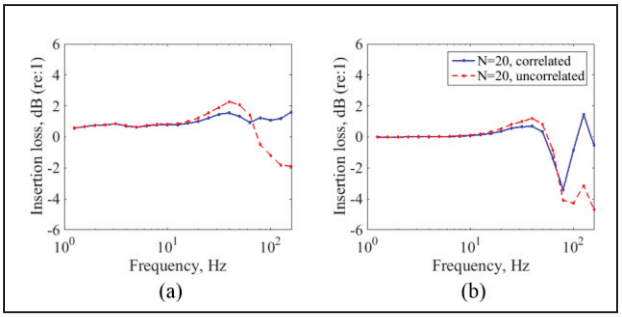

Figure 8. Insertion loss at $y = 0$ (a) and $y = 16$ m (b).

Figure 8, shows the comparison between the predicted pass-by PSD of the dynamic ground response at the track centre-line ($y = 0$) and at distance $y = 16$ m from the track. The results are presented in terms of the insertion loss (IL): i) between the ground velocity levels predicted from the model with homogenous track/ground interface conditions ($N = 1$) and the ground velocity levels predicted from the model with $N = 20$ strip track/ground interface conditions using fully correlated rail roughness input in both cases and ii) between the ground velocity levels predicted from the model with homogenous track/ground interface conditions ($N = 1$) using fully correlated rail roughness input and the ground velocity levels predicted from the model with $N = 20$ strip track/ground interface conditions and using uncorrelated rail roughness input for the two rails. The comparison shows that the models show good agreement for frequencies bellow 70 Hz. For this range of frequencies, their difference is smaller than 1 dB and their performance show the same trends compared with the $N = 1$ model. At higher frequencies the level of vibration predicted using the uncorrelated input drops significantly and the difference between the two models can raise up to 3.5 dB below the track and 4.5 dB at distance $y = 16$ m from the track.

5. Conclusions

The paper highlights the effect of the commonly used assumption in modelling of ground-borne vibration generation that the unevenness of the two rails can be treated as correlated inputs. The traction variation across the track-ground interface was included in the modelling and the track was discretised laterally including both rails. The numerical application showed that the loading interface assumptions can influence significantly the predictions especially at higher frequencies and close to the Rayleigh wavelengths of the soil. Moreover, it was shown that assuming that the loading on the two rails is correlated, the pitching motion of the sleeper is not taken into consideration which can be important for predicting the response at the higher frequencies.

Acknowledgement

This work has been supported by the EPSRC under the research grant EP/K006002/1, "MOTIV: Modelling of Train Induced Vibration".

References

[1] G. Lombaert, G. Degrande, S. Francois, D.J. Thompson: Ground-borne vibration due to railway traffic. IWRN11, Uddevalla, Sweden (2013) 266-301.

[2] M.J.M.M. Steenbergen, A.V. Metrikine: The effect of the interface conditions on the dynamic response of a beam on a half-space to a moving load. European Journal of Mechanics A/Solids, 26 (2007) 33–54.

[3] D.J. Thompson: Railway Noise and Vibration: Mechanisms, Modelling and Means of Control, Elsevier, UK, 2008 (1st ed.).

[4] X. Sheng, C.J.C. Jones, D.J. Thompson: A theoretical model for ground vibration from trains generated by vertical track irregularities. Journal of Sound and Vibration, 272(3-5) (2004) 937–965.

[5] X. Sheng, C.J.C. Jones, M. Petyt: Ground vibration generated by a load moving along a railway track. Journal of Sound and Vibration 228 (1), (1999) 129–156.

[6] E. Ntotsios, M.F.M. Hussein, D.J. Thompson: A comparison between two approaches for calculating power spectral densities of ground-borne vibration from railway trains. EURODYN 2014, Porto, Portugal (2014) 775-782.